Motion Planning for Dynamic Variable Inertia Mechanical Systems with Non-holonomic Constraints

Elie A. Shammas, Howie Choset, and Alfred A. Rizzi

Carnegie Mellon University, The Robotics Institute
Pittsburgh, PA 15213, U.S.A.
eshammas@andrew.cmu.edu, choset@cs.cmu.edu, arizzi@cs.cmu.edu

Abstract: In this paper, we address a particular flavor of the motion planning problem, that is, the gait generation problem for underactuated variable inertia mechanical systems. Additionally, we analyze a rather general type of mechanical systems which we refer to as mixed systems. What is unique about this type of mechanical system is that both non-holonomic velocity constraints as well as instantaneous conservation of the generalized momentum variables defined along the allowable motion direction completely specify the systems velocity.

By analyzing this general type of mechanical systems, we lay the grounds for a general and intuitive analysis of the gait generation problem. Through our approach, we provide a novel framework not only for classifying different types of mechanical systems, but also for identifying a partition on the space of allowable gaits.

By applying our techniques to mixed systems which according to our classification are the most general type of mechanical systems, we verify the generality and applicability of our approach. Moreover, mixed systems yield the richest family of allowable gaits, hence, superseding the gait generation problem for other simpler types of mechanical systems. Finally, we apply our analysis to a novel mechanical system, the *variable inertia snakeboard*, which is a generalization of the original snakeboard that was previously studied in the literature.

1 Introduction

It is straight forward to analyze the motion of a mechanical system due to a particular set of inputs or generalized forces. In fact, this is done by solving a set of second order non-linear differential equations of motion, usually referred to as the Euler-Lagrange equations of motion. In most cases, the solution of this set of differential equations is numerically computed, since in general they do not yield a closed form solution. The gait generation problem involves solving the reverse problem, that is, finding a set of inputs that will cause a desired behavior of motion of the mechanical system. Given, the highly non-linear nature of the governing equations of motion, one can appreciate the

difficulty and complexity of the gait generation problem for mechanical systems. To further complicate the gait generation problem, we gear our analysis toward underactuated mechanical systems, that is, systems that do not have as many actuators as the number of degrees of freedom. Finally, we also seek to verify the generality of our gait generation techniques by analyzing, according to our classification, the most general type of mechanical systems and by ensuring that the systems do not benefit from a fixed inertia property which considerably simplifies the expressions of the equations of motion.

In our prior work, we unified the gait generation approach for two seemingly different families of mechanical systems, *principally kinematic* and *purely mechanical* systems in [12] and [14], respectively. Even though, these two families of systems belong to the opposite ends of a spectrum where at one end are purely mechanical systems whose motion is governed solely by the conservation of momentum while at the other end are principally kinematic systems whose motion is governed solely by the existence of a set of independent non-holonomic constraints that fully constrain the systems velocity, we devised a rather simple gait evaluation tool which is equally applicable to both types of systems. The fact that we proved that momentum, is null for the case of purely mechanical systems and non-existent for the case of the principally kinematic systems allowed us to intuitively generate *geometric* gaits for both systems.

Nonetheless, for mixed system, in general we can not neglect the system's momentum as it could be the dominating contributing factor of motion for certain gaits. At the core of our dynamic gait analysis is a deep understanding of a generalized notion of the systems momentum and its time evolution. We attain this goal through a twofold reduction or simplification of the equations of motion. First, as shown in the prior work, we utilize the symmetry in the laws of physics to represents the evolution of the momentum as a first order differential equation. Additionally, we devised a second reduction step to further simplify the expression of this evolution equation so that we can use to intuitively generate dynamic gaits.

In this paper, we generate gaits for a novel mechanical system, the *variable inertia snakeboard*, shown in Fig. 1(a). This system is a generalization of the *original snakeboard*, (Fig. 1(b)), which was extensively studied in the literature, [2, 8], and which we analyzed in [13]. Both snakeboards belong to the mixed type systems, that is, the non-holonomic constraints do not fully span the fiber space. Thus, the generalized non-holonomic momentum must be instantaneously conserved along certain directions which for the above snakeboards are rotations about the wheel axes intersections. However, the inertia of the original snakeboard is independent of the base variables[1] which greatly simplifies the gait generation analysis. Thus, we consider the variable inertia

[1] Changing the base variables, rotor and wheel axes angles, in Fig. 1(b) will neither change the position of the system's center of mass, nor change its inertia about that point.

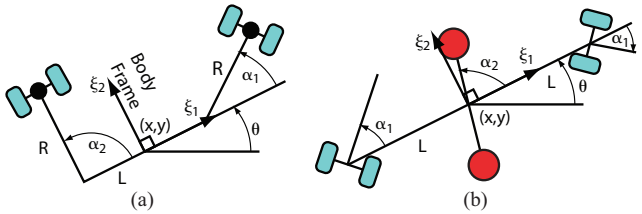

Fig. 1. A schematic of the variable inertia snakeboard in (*a*) and original snakeboard in (*b*) depicting their configuration variables.

snakeboard, which as its name suggests, has a non-constant inertia, to verify the generality and applicability of our gait analysis techniques.

Utilizing our gait generation techniques we design curves in the actuated *base space* which represents the internal degrees of freedom of the robot to translate and rotate the variable inertia snakeboard in the plane. In other words, we will generate gaits by using the actuated base variables to control the un-actuated variables of the *fiber space* which denote the "position" of the system with respect to a fixed inertial frame. Thus, our goal is to design cyclic curves in the base space, which after a complete cycle, produce a desired motion along a specified fiber direction, hence, effectively moving the robot to a new position. We start by presenting the following related prior approaches.

Sinusoidal inputs: Ostrowski *et. al.* expressed the dynamics of a mechanical system in body coordinates and were able to represent it as an affine non-linear control system. Then by taking recourse to control theory, they were able to design *sinusoidal* gaits and specify the gait frequencies. Nonetheless, the gait amplitudes were empirically derived [9]. Ostrowski *et. al.* used their gait generation analysis to generate gaits for the original snakeboard (Fig. 1(b)) [8]. Moreover, Chitta *et. al.* developed several unconventional locomoting robots, such as the robo-trikke and the rollerblader, [4, 10], then used Ostrowski's techniques to generate sinusoidal gaits for these novel locomoting robots. Prior work related to Ostrowski's can also be found in [1, 7, 15].

Kinematic reduction: The work done by Bullo *et. al.* in [3] on kinematic reduction of simple mechanical systems is closely related to our work. They define a kinematic reduction for simple mechanical systems, or in other words, reduce the dynamics of a system so that it can be represented as a kinematic system. Then they study the controllability of these reduced systems and for certain examples, they were able to generate gaits for these systems. In fact, Bullo *et. al.* have designed gaits for the original snakeboard (Fig. 1(b)) which we analyzed in [13]. In this paper, we introduce one type of gait, *a purely kinematic gait*, which is structurally similar to gaits proposed by Bullo *et. al.* in [2]; however, we have a different way of generating these gaits.

2 Background Material

Here we present a rather abbreviated introduction to Lagrangian mechanics, introduce *mixed systems*, and finally we present several mechanics of locomotion results which we shall utilize to generate gaits for mixed systems.

Lagrangian mechanics: The n-dimensional configuration space of a mechanical system, usually denoted by Q, is a trivial principal fiber bundle; that is, $Q = G \times M$ where G is the fiber space which has a Lie group structure and M is the base space. In this paper we assume the Lagrangian of a mechanical system to be its kinetic energy. Moreover, we assume that the non-holonomic constraints that are acting on the mechanical system can be written in a Pfaffian from, $\omega(q) \cdot \dot{q} = 0$, where $\omega(q)$ is a $k \times n$ matrix and $\dot{q}$ represents an element in the tangent space of the configuration manifold Q.

Associated with the Lie group structure of the fiber space, G, we can define the action, Φ_g, and the lifted action, $T_g\Phi_g$, which act on the entire configuration manifold, Q, and tangent bundle, TQ, respectively. Since we can verify that both the Lagrangian and non-holonomic constraints are invariant with respect to these action, we can express the system's dynamics at the Lie group identity[2] as was shown in [5]. In other words, we eliminate the dependence on the placement of the inertial frame. This invariance allows us to compute the *reduced Lagrangian*, $l(\xi, r, \dot{r})$, which according to [8] will have the form shown in (1) and the *reduced non-holonomic constraints* shown in (2) as we demonstrated in [12].

$$l(\xi, r, \dot{r}) = \frac{1}{2} \begin{pmatrix} \xi \\ \dot{r} \end{pmatrix}^T \tilde{M} \begin{pmatrix} \xi \\ \dot{r} \end{pmatrix} = \frac{1}{2} \begin{pmatrix} \xi \\ \dot{r} \end{pmatrix}^T \begin{pmatrix} I(r) & I(r)A(r) \\ A^T(r)I^T(r) & \tilde{m}(r) \end{pmatrix} \begin{pmatrix} \xi \\ \dot{r} \end{pmatrix} \quad (1)$$

$$\bar{\omega}(r) \begin{pmatrix} \xi \\ \dot{r} \end{pmatrix} = \begin{pmatrix} \bar{\omega}_\xi(r) \; \bar{\omega}_r(r) \end{pmatrix} \begin{pmatrix} \xi \\ \dot{r} \end{pmatrix} = 0 \quad (2)$$

Here $\tilde{M}$ is the reduced mass matrix, $A(r)$ is the local form of the mechanical connection, $I(r)$ is the local form of the locked inertia tensor, that is, $I(r) = \mathbb{I}(e, r)$[3], and $m(r)$ is a matrix depending only on base variables. Finally, recall that ξ is an element of the Lie algebra and is given by $\xi = T_g L_{g^{-1}} \dot{g}$, where $T_g L_{g^{-1}}$ is the lifted action acting on a tangent space element $\dot{g}$.

Mixed systems: Such systems are a general type of dynamic mechanical system that are subject to a set of non-holonomic constraints which are invariant with respect to the Lie group action. Hence, a mechanical system whose configuration space has a trivial principal fiber structure, $Q = G \times M$, and is subjected to k non-holonomic constraints, $\omega(q) \cdot \dot{q} = 0$, is said to be *mixed* if the number of constraints acting on it is less than the dimension of

[2] Note that the elements of the tangent space at the fiber space identity form a Lie algebra which is usually denoted by $\mathfrak{g}$.

[3] e is the Lie group identity element.

the system's fiber space ($0 < k < l$), the constraints are linearly independent ($\det(\omega(q)) \neq 0$), and the constraints are invariant with respect to the Lie group actions ($\omega(q) \cdot \dot{q} = \omega(\Phi_g(q)) \cdot T_g\Phi_g(\dot{q}) = 0$).

Mechanics of locomotion: Now we borrow some well-known results from the mechanics of locomotion, [6], upon which we shall build our own gait generation techniques. For a mixed system, according to [8] the system's configuration velocity expressed in body coordinates, ξ, is given by the *reconstruction* equation shown in (3), where $\mathbf{A}(r)$ is an $l \times m$ matrix denoting the local form of the *mixed non-holonomic connection*, $\Gamma(r)$ is an $l \times (l-k)$ matrix, and p is the generalized non-holonomic momentum. We can compute this momentum variable by $p = \frac{\partial l}{\partial \xi}\bar{\Omega}^T$ where $\bar{\Omega}^T$ is a basis of $\mathcal{N}(\bar{\omega}_\xi)$, the null space of $\bar{\omega}_\xi$. Then using (1) we compute the expression for p as shown in (4).

$$\xi = -\mathbf{A}(r)\dot{r} + \Gamma(r)p^T \tag{3}$$

$$p^T = \bar{\Omega}\frac{\partial l}{\partial \xi} = \bar{\Omega}\left(I\xi + IA\dot{r}\right) = \begin{pmatrix} \bar{\Omega}I & \bar{\Omega}IA \end{pmatrix}\begin{pmatrix} \xi \\ \dot{r} \end{pmatrix} \tag{4}$$

$$\dot{p} = p^T\sigma_{pp}(r)p + p^T\sigma_{p\dot{r}}(r)\dot{r} + \dot{r}^T\sigma_{\dot{r}\dot{r}}(r)\dot{r} \tag{5}$$

Moreover, for systems with a single generalized momentum variable[4], its evolution is governed by a first order differential equation[5] shown in (5), where the σ's are matrices of appropriate dimensions whose components depend solely on the base variables. Later in the paper, we will utilize both (3) and (5) and rewrite them in appropriate forms that will help us generate gaits.

Example: Now we introduce our example system, the variable inertia snakeboard, which is composed of three rigid links that are connected by two actuated revolute joints as shown in Fig. 1(a). The outer two links have mass, m, concentrated at the distal ends and an inertia, j, while the middle link is massless. Moreover, attached to the distal ends of the outer two links is a set of passive wheels whose axes are perpendicular to the robot's links. The no sideways slippage of these two sets of wheels provide the two non-holonomic constraints which act on the system.

We attach a body coordinate frame to the middle of the center link and align its first axis along that link. The location of the origin of this body attached frame is represented by the configuration variables (x, y) while its orientation is represented by the variable θ. The two actuated internal degrees of freedom are represented by the relative inter-link angles (α_1, α_2).

Hence, the variable inertia snakeboard has a five-dimensional ($n = 5$) configuration space $Q = G \times M$, where the associated Lie group fiber space

[4] For systems with more than one momentum variables, (5) will be a systems of differential equations involving tensor operations as was shown in [1, 5].

[5] Recall that these equations are the dynamic equations of motion along the fiber variables expressed using the generalized momentum variables.

denoting the robot's position and orientation in the plane is $G = SE(2)$, the special Euclidean group. The base space denoting the internal degrees of freedom is $M = \mathbb{S} \times \mathbb{S}$. The Lagrangian of the variable inertia snakeboard in the absence of gravity is computed using $L(q, \dot{q}) = \frac{1}{2} \sum_{i=1}^{3} (m_i \dot{x}_i^T \dot{x}_i + j_i \dot{\theta}_i^2)$. Let $2L$ and R be the length of the middle link and the outer links, respectively. Moreover, to simplify some expressions we assume that the mass and inertia of the two distal links are identical, that is, $m_i = m$ and $j_i = j = mR^2$. Given that the fiber space has an $SE(2)$ group structure, we can compute the body velocity representation of a fiber velocity where we have $\xi = T_g L_{g^{-1}} \dot{g}$, that is $\xi^1 = \cos(\theta)\dot{x} - \sin(\theta)\dot{y}$, $\xi^2 = \sin(\theta)\dot{x} + \cos(\theta)\dot{y}$, and $\xi^3 = \dot{\theta}$.

$$I = mR \left(\begin{array}{c|c|c} \frac{2}{R} & 0 & -\sin(\alpha_1) + \sin(\alpha_2) \\ 0 & \frac{2}{R} & \cos(\alpha_1) - \cos(\alpha_2) \\ -\sin(\alpha_1) + \sin(\alpha_2) & \cos(\alpha_1) - \cos(\alpha_2) & \frac{L^2+2R^2}{R/2} + \frac{\cos(\alpha_1)+\cos(\alpha_2)}{1/2L} \end{array} \right) \quad (6)$$

$$IA = mR \begin{pmatrix} -\sin(\alpha_1) & \sin(\alpha_2) \\ \cos(\alpha_1) & -\cos(\alpha_2) \\ 2R + L\cos(\alpha_1) & 2R + L\cos(\alpha_2) \end{pmatrix} \text{ and } \tilde{m} = mR \begin{pmatrix} 2R & 0 \\ 0 & 2R \end{pmatrix} \quad (7)$$

$$\bar{\omega}_\xi = \begin{pmatrix} -\sin(\alpha_1) & \cos(\alpha_1) & R + L\cos(\alpha_1) \\ \sin(\alpha_2) & -\cos(\alpha_2) & R + L\cos(\alpha_2) \end{pmatrix} \text{ and } \bar{\omega}_r = \begin{pmatrix} R & 0 \\ 0 & R \end{pmatrix} \quad (8)$$

The above transformation allows us to verify the Lagrangian invariance and to compute the reduced Lagrangian. Thus, the components of the reduced mass matrix as is shown in (1) are given in (6) and (7). Note that the reduced mass matrix is not constant as was the case for the original snakeboard [13] and it depends solely on the base variables, α_1 and α_2. Similarly we can write the non-holonomic constraints in body coordinates for the variable inertia snakeboard where the components of (2) are given in (8). Moreover, note that the variable inertia snakeboard has a three-dimensional fiber space, $SE(2)$, and it has two non-holonomic constraints, one for each wheel set. We have verified that these constraints are invariant with respect to the group action and we know that these non-holonomic constraints are linearly independent away from singular configurations. Thus, we conclude that the variable inertia snakeboard a *mixed* type system.

Using the above computed components of the reduced mass matrix in (6) and (7) and the non-holonomic constraints in (8), we can easily compute the *reconstruction* equation shown in (3) and the generalized non-holonomic momentum as shown in (4). For the sake of brevity, we will not present the explicit structure of these expressions. Finally, utilizing the generalized non-holonomic momentum and the reconstruction equations, we can rewrite the original Euler-Lagrange equations of motion in terms of the generalized non-holonomic momentum to arrive at the *momentum evolution* equation, (5).

3 Scaled Momentum

Rewriting the system dynamics in terms of the generalized non-holonomic momentum yields a rather simple expression of the equations of motion as shown in (3) and (5). Nonetheless, we can clearly see that the generalized momentum is not zero for all time as was the case purely mechanical systems, thus, when we integrate the reconstruction equation the second dynamic, $\Gamma(r)p^T$ term does not vanish. Analyzing this dynamic term is rather complicated since one can not solve for the generalized momentum in a closed from. In fact, Bullo *et. al.* avoided this computing second term by considering gaits that nullify it. We, on the other hand, will introduce a new momentum variable that will simplify the dynamic terms analysis which will allow us to generate a richer family of gaits.

Now we manipulate (5) to a more manageable form which allows us to intuitively evaluate the dynamic phase shift. At this point we will limit ourselves to systems that have one less velocity constraint than the dimension of the fiber space, i.e., $l-k=1$. This assumption leaves us with only one generalized momentum variable and forces the term $\sigma_{pp}(r)=0$ in (5) as was explained in [8]. Moreover, first order differential equation theory confirms that an integrating factor, $h(r)$, exists for (5). Hence, the assumption $l-k=1$ allows us to easily find a closed form solution for the integrating factor for the momentum evolution equation (5). In our future work, we will address the existence of this integrating factor for systems for which the above assumption does not hold. Thus, we define the scaled momentum as $\rho = h(r)p$ and rewrite (3) and (5) to arrive at

$$\xi = -\mathbf{A}(r)\dot{r} + \bar{\Gamma}(r)\rho, \text{ and} \tag{9}$$

$$\dot{\rho} = \dot{r}^T \bar{\Sigma}(r)\dot{r}, \tag{10}$$

where $\bar{\Gamma}(r) = \Gamma(r)/h(r)$ and $\bar{\Sigma}(r) = h(r)\sigma_{\dot{r}\dot{r}}(r)$. Now that we have written the reconstruction and momentum evolution equations in our simplified forms shown in (9) and (10), we are ready to generate gaits by studying and analyzing the three terms, $\mathbf{A}(r)$, $\bar{\Gamma}(r)$, and $\bar{\Sigma}(r)$. In fact, we will use $\mathbf{A}(r)$ and $\bar{\Gamma}(r)$ to respectively construct the *height* and *gamma* functions while we use $\bar{\Sigma}(r)$ to study the sign definiteness of the scaled momentum.

4 Gait evaluation

In this section, we equate the position change due to any closed base-space curve to *two* decoupled terms. Then, we present how to design curves in such a way to *exclusively* ensure that any of these terms is non-zero along a specified fiber direction, that is, effectively synthesizing two types of gait associated with each of the decoupled terms. In the next section, we will define

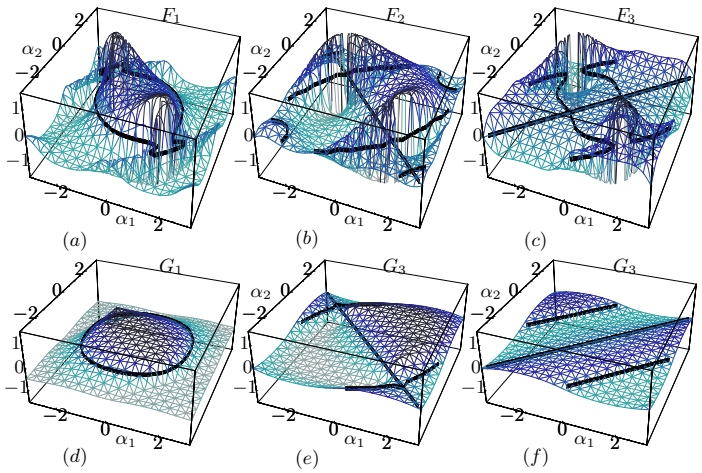

Fig. 2. The three height functions, (F_1, F_2, F_3), and three gamma functions, (G_1, G_2, G_3), corresponding to the three fiber directions in body representation, (ξ_1, ξ_2, ξ_3), for the variable inertia snakeboard are depicted in (a) through (f). The darker colors indicate the positive regions which are separated by solid lines from the lighter colored negative regions.

a partition on the space of allowable gaits such that we can generate gaits by relating position change to either one of the decoupled terms or both. For the first case, we exclusively use the gait synthesis tools presented in this section while for the second case we define another type of gaits that simultaneously utilizes both gait synthesis tools.

We define a *gait* as a closed curve, ϕ, in the base space, M, of the robot. We require that our gaits be cyclic and continuous curves. Having written the body representation of a configuration velocity in a simplified manner as seen in (9), we solve for position change by integrating (9). Defining ζ as the integral of ξ and then integrating each row of (9) with respect to time we get

$$\begin{aligned}\Delta\zeta^i &= \int_{t_0}^{t_1} \dot{\zeta}^i dt = \int_{t_0}^{t_1} \xi^i dt = \int_{t_0}^{t_1} \left(-\sum_{j=1}^{m} \mathbf{A}^i_j(r)\dot{r}^j + \sum_{j=1}^{l-k} \bar{\Gamma}^i_j(r)\rho^j \right) dt \\ &= \underbrace{\int\int_{\Phi} \sum_{o,j=1,o<j}^{m} \bar{\mathbf{A}}^i_{oj}(r) dr^o dr^j}_{I^{GEO}} + \underbrace{\int \sum_{j=1}^{l-k} \left(\bar{\Gamma}^i_j(r) \int \left(\dot{r}^T \bar{\Sigma}(r) \dot{r} \right)^j dt \right) dt}_{I^{DYN}} \quad (11)\end{aligned}$$

Note that the first term can be written as a line integral and then by using Stokes' theorem we equate it to a volume integral. As for the second term we just substitute for the scaled momentum, ρ, using (10). Hence, we equated position change to two integrals, I^{GEO} which computes the geometric phase

shift and I^{DYN} which computes the dynamic phase shift. Next, we analyze how to synthesize gaits using the two independent phase shifts.

4.1 Evaluating geometric gaits

For simplicity, we limit ourselves to two-dimensional base spaces, that is, ($m = 2$). This allows us to equate the *geometric* position change contribution, I^{GEO}, due to any gait, ϕ, by computing the volume integral $\int\int_{\phi} F^i(r^1, r^2)dr^1dr^2$, where $F^i = \frac{\partial A_2^i}{\partial r_1} - \frac{\partial A_1^i}{\partial r_2}$'s are the well-defined *height function* associated with the fiber velocity ξ^i. Then, we generate *geometric gaits* by studying certain properties of the height functions: *Symmetry* to study smaller portions of the base space, *Signed regions* to control the orientation of the designed curves as well as the magnitude of the the geometric phase shift, and *Unboundedness* to identify singular configurations of the robot.

By inspecting the above properties of the height functions we are able to easily design curves that only envelope a non-zero volume under a desired height function while it encloses zero volume under the rest of the height functions. For example, *Closed non-self-intersecting curves* that stay in a single signed region are guaranteed to enclose a non-zero volume and *Closed self-intersecting curves* that span two regions with opposite signs and that change orientation as they pass from one region to another are also guaranteed to enclose a non-zero volume. On the other hand, *Closed non-self-intersecting curves that are symmetric about odd points* are guaranteed to have zero volume and *Closed self-intersecting curves that are symmetric about even points* are guaranteed to have zero volume. Note that these rules do not impose any additional constraints on the shape of the input curves.

4.2 Evaluating dynamic gaits

Now, we will analyze the second term in (11), to propose gaits that ensure that I^{DYN} is non-zero along a desired fiber direction. Note that for each fiber direction the integrand of I^{DYN} in (11) is composed of the product of two terms, the *gamma function*, $\bar{\Gamma}^i(r)$, and the scaled momentum variable, ρ. Thus, by analyzing the $\bar{\Sigma}$ matrix in (11) we propose families gaits that ensure that the scaled momentum variable is sign-definite. Then, we analyze the the gamma functions in a similar way to how we analyze the height functions, that is, we study their symmetry, signed regions, and unbounded regions. Note that, we do not use Stokes' theorem on the gamma functions as we did for the height functions, since the dynamic phase shift is equated to a time definite integral not to a path integral as was the case for the geometric phase shift. Thus, by picking gaits that are located in a same signed region of $\bar{\Gamma}^i(r)$, we ensure the integrand of I^{DYN} is non-zero along a desired fiber direction.

Example: Now we compute the height and gamma functions for the variable inertia snakeboard. The expressions for this particular system are rather

complicated and we will not present them in this paper; however, the expressions can be found in [11] and we depict the graphs of the three height and gamma functions in Fig. $2(a)-(c)$ and $(d)-(f)$, respectively. These functions have the following properties which we will utilize later to generate gaits.

- $F_2 = G_2 = 0$ for $\alpha_1 = -\alpha_2$,
- $F_3 = G_3 = 0$ for $\alpha_1 = \alpha_2$,
- F_1 and G_1 are even about both lines $\alpha_1 = \alpha_2$ and $\alpha_1 = -\alpha_2$,
- F_2 and G_2 are even about $\alpha_1 = \alpha_2$ and odd about $\alpha_1 = -\alpha_2$,
- F_3 and G_3 are odd about $\alpha_1 = \alpha_2$ and even about $\alpha_1 = -\alpha_2$.

5 Gait generation for mixed system

In this section, we utilize our geometric and dynamic gait synthesis to generate gaits for mixed systems. Next, we define a partition on the allowable gait space which allows us to independently analyze I^{GEO} and I^{DYN} and generate gaits using our synthesis tools. We respectively label the two families of gaits as *purely kinematic* and *purely dynamic* gaits. Moreover, we propose a third type of gait that simultaneously utilizes both shifts, I^{GEO} and I^{DYN}, to produce motions with relatively larger magnitudes. We label this family of gaits as *kino-dynamic* gaits.

5.1 Purely kinematic gaits

Purely kinematic gaits are gaits whose motions is solely due to I^{GEO}, that is, $I^{DYN} = 0$ for all time. A solution for such a family of gaits is to set $\rho = 0$ in (11) which sets the integrand of I^{DYN} to zero. Thus, we define purely kinematic gaits as gaits for which $\rho = 0$ for all time. Note that for purely mechanical systems $p = \rho = 0$ by definition and for principally kinematic systems $I^{DYN} = 0$ since $p = \varnothing$. Hence, any gait for these two types of systems is necessarily purely kinematic. However, for mixed systems, we generate purely kinematic gaits by the following two step process:

- Solving the scaled momentum evolution equation, (10), for which $\rho = \dot{\rho} = 0$. This step defines vector fields over the base space whose integral curves are candidate purely kinematic gaits.
- Using our geometric gait synthesis analysis on the above candidate gaits to concatenating parts of integral curves that enclose a non-zero volume under the desired height functions.

Sometimes, purely kinematic gaits are referred to as *geometric* gaits, since the produced motion is solely due to the generated geometric phase as defined in [1]. Moreover, purely kinematic gaits are structurally similar to gaits proposed by Bullo in his kinematic reduction of mechanical systems in [3].

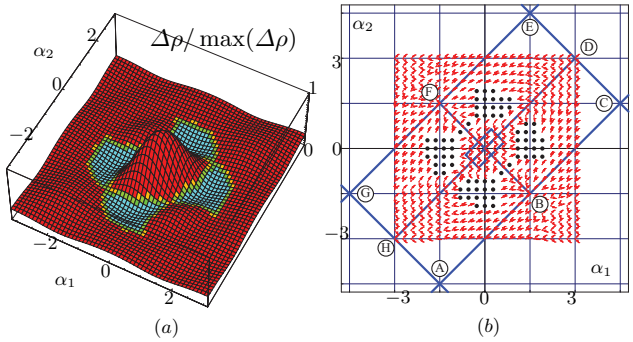

Fig. 3. (a) Plot indicating the negative regions (lighter colored regions) of the base space where $\Delta\rho < 0$. (b) Two vector fields defined over the base space whose integral curves are purely kinematic gaits. The solid lines are integral curves of the vector fields which we will utilize to generate purely kinematic gaits. The solid dots indicate the negative regions of $\Delta\rho$ where the vector fields are not defined.

The vector fields defined above essentially serve the same purpose of the decoupling vector fields presented in Bullo's work.

Example: For the variable inertia snakeboard, we can easily design purely kinematic gaits by solving for the right hand side of (10) equal to zero. Since the right hand side of (10) is a quadratic in the base velocites[6], we ensure that the term $\Delta\rho(\alpha_1, \alpha_2) = \bar{\Sigma}_1^2\bar{\Sigma}_1^2 - \bar{\Sigma}_1^1\bar{\Sigma}_2^2 \geq 0$. A plot of a $\Delta\rho/\max(\Delta\rho)$ is shown in Fig. 3(a). The light colored regions indicate that $\Delta\rho(\alpha_1, \alpha_2) < 0$, that is, we can never compute any velocities for which $\dot{\rho} = 0$. In other words, we should avoid these regions of the base space while designing purely kinematic gaits.

Away from the negative regions of $\Delta\rho(\alpha_1, \alpha_2)$, we design purely kinematic gaits for the variable inertia snakeboard. The right hand side of (10) has four unknowns, $(\alpha_1, \alpha_2, \dot{\alpha}_1, \dot{\alpha}_2)$. Thus, at each point in the base space, that is, fixing (α_1, α_2), we need to solve the velocities $(\dot{\alpha}_1, \dot{\alpha}_2)$ for which the right hand side is zero. Since, we have two unknowns and one equation, we solve for the ratios, $\frac{\dot{\alpha}_1}{\dot{\alpha}_2}$ and $\frac{\dot{\alpha}_2}{\dot{\alpha}_1}$ for which the right hand side is zero. Thus, ignoring the magnitudes of the base velocities, the two ratios $\frac{\dot{\alpha}_1}{\dot{\alpha}_2}$ and $\frac{\dot{\alpha}_2}{\dot{\alpha}_1}$ define the slopes of vectors at each point in the base space which we use to define vector fields over the entire base space as depicted in Fig. 3(b). Hence, any part of an integral curve of the above vector fields is necessarily a purely kinematic gait. For example, the families of lines, $l_1 = \{\alpha_2 = \alpha_1 + k\pi, k \in \mathbb{Z}\}$ and $l_2 = \{\alpha_2 = -\alpha_1 + 2k\pi, k \in \mathbb{Z}\}$ are the simplest integral curves we could define whose velocities exactly match the above vector fields.

[6] For the original snakeboard, we verified in [13] that the right hand side of the scaled momentum evolution equation is not a quadratic. This simplified the generation of purely kinematic gaits and mislead us into believing that purely kinematic gaits could be defined everywhere on the base space.

Purely Kinematic	Purely Dynamic	Kino-dynamic
Polygon $ACEGA$	$\alpha_1 = \frac{\pi}{4}(1 - \sin(t) - 2\sin^2(t))$ $\alpha_2 = \frac{\pi}{4}(1 + \sin(t) - 2\sin^2(t))$	$\alpha_1 = -\frac{1}{\sqrt{2}}\left(\frac{\pi}{2}\sin(t) + \frac{\pi}{4}\cos(t)\right)$ $\alpha_2 = \frac{1}{\sqrt{2}}\left(-\frac{\pi}{2}\sin(t) + \frac{\pi}{4}\cos(t)\right)$
Polygon $ABFECBFGA$	$\alpha_1 = \frac{\pi}{10}(2\sin(3t) - 5)$ $\alpha_2 = \frac{\pi}{6}(\sin(t) - 3)$	$\alpha_1 = \frac{1}{\sqrt{2}}\left(\frac{\pi}{2}\sin(2t) + \frac{\pi}{4}\sin(t)\right)$ $\alpha_2 = -\frac{1}{\sqrt{2}}\left(\frac{\pi}{2}\sin(2t) - \frac{\pi}{4}\sin(t)\right)$
Polygon $ACDHGEDHA$	$\alpha_1 = \frac{\pi}{4}(2\sin(t) + 1)$ $\alpha_2 = \frac{\pi}{4}(2\sin(t) - 1)$	$\alpha_1 = \frac{1}{\sqrt{2}}\left(\frac{\pi}{3}\sin(2t) + \frac{\pi}{3}\sin(t)\right)$ $\alpha_2 = \frac{1}{\sqrt{2}}\left(-\frac{\pi}{3}\sin(2t) + \frac{\pi}{3}\sin(t)\right)$

Table 1. Three proposed gaits of each family for the variable inertia snakeboard.

To design a purely kinematic gait that will move the variable inertia snakeboard along say the ξ^1 direction, we pick any closed integral curve that will enclose a non-zero volume solely under the first height function. Using the above lines, we know that the polygon given in the first row of the first column of Table 1 and depicted in Fig. 3(b) will move the snakeboard along the ξ_1 direction. Similarly we construct two other polygons shown in the second and third rows of the first column of Table 1 as depicted in Fig. 3(b) to respectively locomote the snakeboard along the ξ_2 and ξ_3 directions.

Inspecting the above polygonal gaits, we found out that they pass through the snakeboard's singular configurations, $(\alpha_1, \alpha_2) = \{(\frac{\pi}{2}, -\frac{\pi}{2}), (-\frac{\pi}{2}, \frac{\pi}{2})\}$, (Fig. $2(a) - (c)$). So rather than solving numerically for other integral curves of the vector fields and solve for other possible gaits which is a tedious process, we simply shrunk the above proposed gaits around the center of the base space as shown in Fig. 3(b). These curves closely, but not exactly, match the vector fields. So we shall expect a change in the scaled momentum value as we traverse these gaits since they are an approximate solution. The motions of the variable inertia snakeboard due to these gaits are depicted in Fig. $4(a) - (c)$. Note, the small magnitudes of motion due to the small volumes under the height functions. However, we can clearly see that the gaits move the variable inertia snakeboard along the x and y directions in Fig. $4(a)$ and Fig. $4(b)$, respectively, and rotate the snakeboard in Fig. $4(c)$.

Finally, recall that, our analysis is done in body coordinates, ξ^i's, which are related by the map $T_g L_{g^{-1}}$ to the fiber variables, $\dot{g}^i$'s. Since, the fiber space for the variable inertia snakeboard is $SE(2)$ which is not Abelian, the map $T_g L_{g^{-1}}$ is non-trivial; hence, one should not expect a direct correspondence between say ξ^1 and $\dot{x}$. This explains the non-pure fiber motions in Fig. $4(a)$, where motion along ξ^1 transforms to major motion along x and minor motion along the y axis.

5.2 Purely dynamic gaits

As the name suggests, purely dynamic gaits are gaits that produce motion solely due to the dynamic phase shift, that is, $I^{GEO} = 0$ while $I^{DYN} \neq 0$. These gaits are relatively easy to design since these are gaits that enclose no

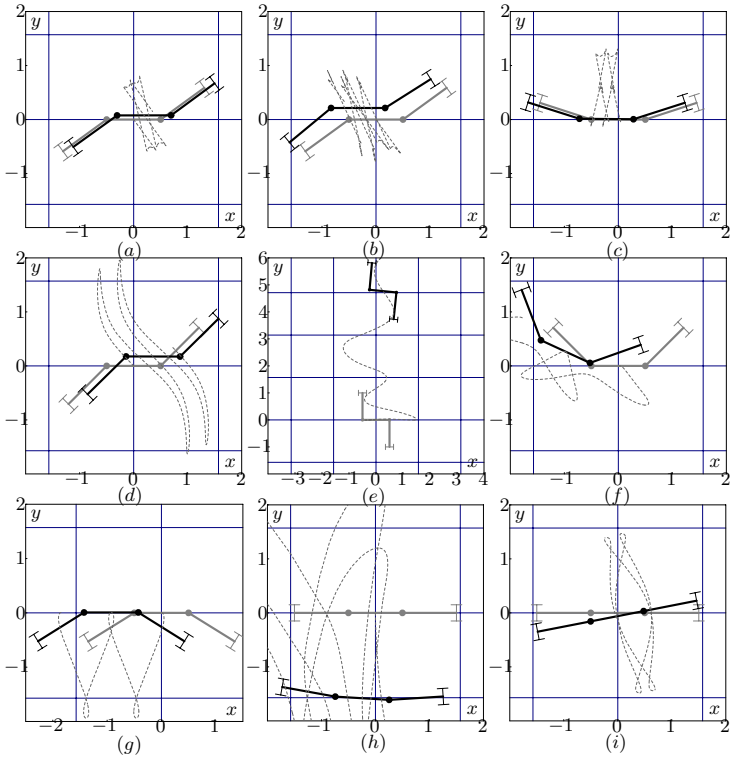

Fig. 4. The actual motion that the variable inertia snakeboard will follow as the base variables follow the three *purely kinematic* depicted in the first column of Table 1 shown respectively in a, b, and c; three *purely dynamic* gaits depicted in the second column of Table 1 shown respectively in d, e, and f; and three *kino-dynamic* gaits depicted in the third column of Table 1 shown respectively in g, h, and i. The initial and final configurations for each gait are shown in gray and black colors, respectively, while the dotted line depicts the trace of the origin of the body-attached coordinate frame.

"volume" in the base space. Note that all systems that have only *one* base variables have gaits that are necessarily purely dynamic, since setting $m = 1$ in (11) will yield $I^{GEO} = 0$. For example, all the gaits for robo-Trikke robot which was studied by Chitta *et. al.* in [4] are necessarily purely dynamic since there exists only one base variable. As for systems with more than one base space variable, it is still relatively easy to construct purely dynamic gaits. Such gaits do not enclose any area in the base space. A simple solution would be to ensure that a gait retraces the same curve in the second half cycle of the gait but in the opposite direction.

Thus, we propose the following purely dynamic families of gaits: $\{r_1, r_2\} = \{\sum_{i=0}^{n} a_i \left(f(t)\right)^i, f(t)\}$, where $f(t) = f(t+\tau)$ is a periodic real function and

a_i's are real numbers. We can verify that these gaits will have zero area in the base space (r_1, r_2). Moreover, we can verify that for the above family of gaits, the scaled momentum variable is sign-definite, that is, $\rho \leq 0$ or $\rho \geq 0$ for all time. Then, generating purely dynamic gaits reduces to the following simple procedure:

- Select gaits from the above described family and check the sign of the scaled momentum variable ρ.
- Analyze the gamma functions depicted in (9) and (11) to pick the gait that ensures that the integrand of I^{DYN} is non-zero for the desired fiber direction.

Example: For the variable inertia snakeboard, we construct three purely dynamic gaits depicted in the second column of Table 1. The motion due to these gaits are respectively shown in Fig. $4(d)-(f)$. For instance, we designed the first gait in the second column of Table 1 such that $\rho \leq 0$ for all time. The gait is located close to the center of the base space and is symmetric about the line $\alpha_1 = -\alpha_2$; moreover, only the first gamma function is non-zero and even about the line $\alpha_1 = -\alpha_2$ while the second and third gamma functions is odd about this line. Thus we expect a non-zero I^{DYN} only along the ξ^1 direction. This motion, is largely transformed to motion along the x direction as shown in Fig. $4(d)$. Similarly, we designed the other two gaits to move the variable inertia snakeboard along the y direction, (Fig. $4(e)$) and to rotate it along the θ direction, (Fig. $4(f)$).

5.3 Kino-dynamic gaits

Finally, we have the third type of gaits which we term as kino-dynamic gaits. These gaits have both I^{GEO} and I^{DYN} not equal to zero, that is, the motion of the system is due to both the geometric phase shift as well as the dynamic phase shift which are associated with I^{GEO} and I^{DYN}, respectively. We design kino-dynamic gaits in a two step process.

- First we do the volume integration analysis on I^{GEO} to find a set of candidate gaits that move the robot in the desired direction.
- The second step it to compute I^{DYN} for the candidate gaits and verify that the effect of I^{DYN} actually enhances the desired motion.

Essentially, kino-dynamic gaits are variations of purely kinematic gaits. In a sense, we start by generating a purely kinematic gait but by neglecting the constraints that the gaits has to be an integral curve of the vector fields that prescribes the purely kinematic gaits. Thus, we know that scaled momentum is not necessarily zero for all time, that is, $I^{DYN} \neq 0$. Then, we pick the gaits for which the magnitude of I^{DYN} additively contribute to that of I^{GEO}, hence, effectively producing fiber motions with bigger magnitudes.

Example: For the variable inertia snakeboard, we can generate kino-dynamic gaits by using the volume integration analysis to produce candidate gaits. For example, to generate a gait that rotates the variable inertia snakeboard in place, we start by designing a curve in the base space that envelopes a non-zero volume only under the third height function of the variable inertia snakeboard (Fig. 2(c)). A figure-eight type curve with each of its loops having opposite orientation and lying on the opposite side of the line $\alpha_1 = \alpha_2$, will envelope non-zero volume only under the third height function. This curve is the last curve in the third column of Table 1. We simulated this proposed gaits and indeed it does rotate the variable inertia snakeboard along the θ direction as shown in (Fig. 4(i)). Similarly, we designed two other curves depicted in the first and second rows of the last column of Table 1 to move the variable inertia snakeboard along the x direction, (Fig. 4(g)), and the y direction ,(Fig. 4(h)).

In this section we have generated three of each type of gaits that moved the variable inertia snakeboard in any specified global direction. Moreover, we have the freedom to choose from several of the types of gaits that we have proposed earlier. It is worth noting that the purely kinematic and purely dynamic gaits were the easiest to design since we are exclusively analyzing either I^{KIN} or I^{DYN} and not both at the same time as is the case for kin-dynamic gaits.

6 Conclusion

In this paper, we studied mixed non-holonomic systems and designed three families of gaits, purely kinematic, purely dynamic, and kino-dynamic gait, to move such systems along specified fiber directions. This work is a generalization over our prior work where we used one type of the gaits defined here to analyze two other systems, purely mechanical and principally kinematic. Moreover, our technique affords better flexibility in choosing the parameters of the suggested gaits and reduces the need for intuition about how to to manually adjust these parameters.

One of the contributions of this paper is the introduction of the scaled momentum variable which greatly simplified our gait generation analysis. This new variable allowed us to rewrite both the reconstruction as well as the momentum evolution equation in simpler forms that are suitable for our gait generation techniques. Another contribution is the introduction of the novel mechanical system, the variable inertia snakeboard. This system is similar enough to the original snakeboard that we can relate our results to this well known system, but at the same time it did not over simplify the gait generation problem. In fact, through analyzing the variable inertia snakeboard, we identified regions in the base space where purely kinematic gaits are not possible. There are no such regions for the original snakeboard.

This paper constitutes a first step towards developing an algorithmic gait synthesis technique. Our next step would be to relax the assumptions we made

such that we can analyze system with more than two-dimensional base spaces and systems with more than one generalized momentum variable. Ideally, we would like to develop an algorithm whose inputs are the system's configuration space structure, its Lagrangian, and the set of non-holonomic constraint acting on the system. The algorithm would automatically generate gaits that will move the system along a desired global direction with a desired magnitude. However, we still need to develop several additional tools to complete this gait generating algorithm.

References

1. A. Bloch. *Nonholonomic Mechanics and Control*. Springer Verlag, 2003.
2. F. Bullo and A. D. Lewis. Kinematic Controllability and Motion Planning for the Snakeboard. *IEEE Transactions on Robotics and Automation*, 19(3):494–498, 2003.
3. F. Bullo and A. D. Lewis. *Geometric Control of Mechanical Systems: Modeling, Analysis, and Design for Simple Mechanical Control Systems*. Springer, 2004.
4. S. Chitta, P. Cheng, E. Frazzoli, and V. Kumar. RoboTrikke: A Novel Undulatory Locomotion System. In *IEEE International Conference on Robotics and Automation*, 2005.
5. J. Marsden. *Introduction to Mechanics and Symmetry*. Springer-Verlag, 1994.
6. J. Marsden, R. Montgomery, and T. Ratiu. Reduction, Symmetry and Phases in Mechanics. *Memoirs of the American Mathematical Society*, 436, 1990.
7. R. M. Murray and S. S. Sastry. Nonholonomic Motion Planning: Steering Using Sinusoids. *IEEE T. Automatic Control*, 38(5):700 – 716, May 1993.
8. J. Ostrowski. *The Mechanics of Control of Undulatory Robotic Locomotion*. PhD thesis, California Institute of Technology, 1995.
9. J. Ostrowski and J. Burdick. The Mechanics and Control of Undulatory Locomotion. *International Journal of Robotics Research*, 17(7):683 – 701, July 1998.
10. V. K. S. Chitta, F. Heger. Dynamics and Gait Control of a Rollerblading Robot. In *IEEE International Conference on Robotics and Automation*, 2004.
11. E. Shammas. *Generalized Motion Planning for Underactuated Mechanical Systems*. PhD thesis, Carnegie Mellon University, March 2006.
12. E. Shammas, H. Choset, and A. Rizzi. Natural Gait Generation Techniques for Principally Kinematic Mechanical Systems. In *Proceedings of Robotics: Science and Systems*, Cambridge, USA, June 2005.
13. E. Shammas, H. Choset, and A. A. Rizzi. Towards Automated Gait Generation for Dynamic Systems with Non-holonomic Constraints. In *IEEE International Conference on Robotics and Automation*, 2006.
14. E. Shammas, K. Schmidt, and H. Choset. Natural Gait Generation Techniques for Multi-bodied Isolated Mechanical Systems. In *IEEE International Conference on Robotics and Automation*, 2005.
15. G. Walsh and S. Sastry. On reorienting linked rigid bodies using internal motions. *Robotics and Automation, IEEE Transactions on*, 11(1):139–146, January 1995.